

# Experimental observation of guided polarized neutrons in magnetic-thin-film waveguides

S. P. Pogossian

CNRS, Laboratoire de Matériaux Isolants, Magnétiques et Semi-conducteurs, 1, Place Aristide Briand, 92195 Meudon, France

A. Menelle

Laboratoire Léon Brillouin, CEA, CNRS, CE Saclay, 91191 Gif-sur-Yvette, France

H. Le Gall, J. M. Desvignes, and M. Artinian

CNRS, Laboratoire de Matériaux Isolants, Magnétiques et Semi-conducteurs, 1, Place Aristide Briand, 92195 Meudon, France

(Received 24 October 1995; revised manuscript received 29 January 1996)

Guided propagation of polarized neutrons has been observed directly in magnetic CoZr/Al/CoZr trilayer deposited on Gd<sub>3</sub>Ga<sub>5</sub>O<sub>12</sub> garnet substrate by using neutron reflectometry technique. The resonance observed in the transmission spectrum of neutrons corresponding to two low order guided modes is in good agreement with theoretical predictions. A detailed theoretical description of the guided propagation in thin-film neutron waveguides is also presented. [S0163-1829(96)04221-X]

## I. INTRODUCTION

Recently several theoretical and experimental works concerning the neutron waveguiding in thin-film structures has been reported.<sup>1-5</sup> The theory of thin-film neutron waveguides (TFNW) of several hundreds angstroms was first proposed by De Wames *et al.*<sup>1</sup> and extended by Pogossian *et al.*<sup>2,4</sup> A direct experimental observation of quasiguided neutron waves was realized by Feng *et al.*<sup>3</sup> In the experimental setup realized by Feng *et al.*<sup>3</sup> only nonbound modes were possible to excite by the in coupling prism since the true bound modes were hidden due to the high refractive index of the coupling gap. In the above mentioned paper<sup>3</sup> an analysis of the reflected wave was also absent. In the present paper we propose an experimental setup whose geometry is similar to that used by Feng *et al.*<sup>3</sup> but the measurement technique is different from the latter. We look for resonances at fixed incident and observation angles by varying the incident neutrons wavelength, while in the setup of Feng *et al.*<sup>3</sup> the angle of incidence was varied for fixed wavelength. In our experiment we observe the neutron guided propagation in a thin film surrounded from both sides by magnetic media. Moreover, the refractive index of the barrier is chosen to be quite low in order to excite the true bound modes. The waveguiding in this structure is selective to the neutron spin, so only one polarization is guided while the oppositely polarized neutrons are attenuated by subsequent reflections from the gadolinium gallium garnet (GGG) absorbing substrate.

Thus we report a direct experimental observation of the guided polarized neutron waves in a TFNW composed of a CoZr/Al/CoZr sandwich on a GGG substrate. The plan of this paper is as follows. In Sec. II we present the necessary theoretical basis for the interpretation of the experimental results. In Sec. III we describe the experimental setup and the results obtained by neutron reflectivity and transmittivity measurements. In Sec. IV we discuss the theoretical and experimental results.

## II. THEORY

As in optics, the reflection and refraction of neutron de Broglie waves in a material can be described by an index of refraction. For nonabsorbing materials the refractive index can be written in the following form:<sup>2</sup>

$$n_j^2(\lambda) = 1 - \lambda^2 \delta_j, \quad (1)$$

where  $\lambda$  is the neutron wavelength,  $\delta_j$  is a constant dependent only on the physical properties of  $j$ th material, and  $n_j - 1$  is of the order of  $10^{-6}$ .

If a thin film of thickness  $h$  and of refraction index  $n_1$  is surrounded from both sides by two media with lower refractive indices  $n_2$  and  $n_3$  ( $n_2, n_3 < n_1$ ), then the neutron de Broglie waves can be guided in the thin film by successive total reflections from the interfaces with two neighboring media. For discrete propagation constants  $\beta_m$ , the neutron waves interfere constructively creating a traveling guided wave in the Al thin guiding film (Fig. 1), which propagates

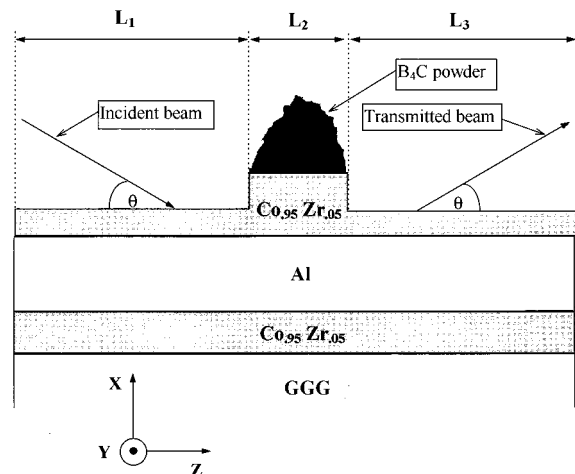


FIG. 1. Representation of the three layered structure deposited on GGG. The lengths  $L_1$ ,  $L_2$ , and  $L_3$  are respectively 29 mm, 6 mm, and 29 mm.

along the  $Z$  axis with the phase term  $\exp(i\beta_m z)$ , where  $i=(-1)^{1/2}$  and  $m=0,1,2$ , etc. Along the  $X$  axis a standing wave is formed. The lateral resonance condition determining the discrete values of  $\beta_m$  is well known from integrated optics:<sup>6-8</sup>

$$2hq_m - 2 \tan^{-1}[(c_2^2 - q_m^2)^{1/2}/q_m] - 2 \tan^{-1}[(c_3^2 - q_m^2)^{1/2}/q_m] = 2\pi m, \quad (2)$$

where  $q_m = k[n_1^2 - (\beta_m/k)^2]^{1/2}$ ,  $c_2 = k[n_1^2 - n_2^2]^{1/2}$ ,  $c_3 = k[n_1^2 - n_3^2]^{1/2}$ , and  $k=2\pi/\lambda$ . If we look for propagation constants in the form

$$(\beta_m/k)^2 = 1 - \lambda^2 a_m, \quad (3)$$

then Eq. (2) for symmetrical waveguides can be written in an elegant form independent from the neutron wavelength:

$$2h(a_m - \delta_1)^{1/2} + (1/\pi) \sin^{-1}\{[(a_m - \delta_1)/(\delta_2 - \delta_1)]^{1/2}\} = m + 1. \quad (4)$$

The constants  $a_m$  determined from Eq. (4) are thus wavelength independent.<sup>2</sup> It is easy to notice that  $q_m$ ,  $c_2$ , and  $c_3$  are also wavelength independent and are expressed by  $\delta_j$  and  $a_m$  as follows:  $q_m = 2\pi[a_m - \delta_1]^{1/2}$ ,  $c_2 = 2\pi[\delta_2 - \delta_1]^{1/2}$ , and  $c_3 = 2\pi[\delta_3 - \delta_1]^{1/2}$ . So the guided and nonguided propagation exhibit similar dispersion properties given by Eqs. (1) and (3). The number  $N$  of guided modes in a symmetrical waveguide ( $n_2 = n_3$ ) of thickness  $h$  is found easily from Eqs. (1) and (2) to be the largest integer smaller than  $1 + 2h(\delta_2 - \delta_1)^{1/2}$ . As can be seen the total number of modes is not dependent on the neutrons wavelength but is determined only by the thickness of the guiding layer and the constants  $\delta_j$ . For low order modes ( $a_m - \delta_1 \ll \delta_2 - \delta_1$ ) Eq. (4) can be approximately written as

$$2h_{\text{eff}}(a_m - \delta_1)^{1/2} = (m + 1), \quad (5)$$

where  $h_{\text{eff}} = h + 1/[\pi(\delta_2 - a_m)^{1/2}] \approx h + 1/[\pi(\delta_2 - \delta_1)^{1/2}]$ .

The neutron waves are coupled into the waveguide by an air prism which has the highest index of refraction compared to those of the guiding film and the surrounding media. In our experimental setup the angle of incidence  $\theta_{\text{inc}}$  is kept constant and the neutron wavelength is varied. So the resonant coupling of incident neutron beam into waveguide modes occurs at resonant wavelengths  $\lambda_m$  satisfying the phase matching condition between the standing waves in the air prism and the quasiguided waves in the guiding film:<sup>2,7,8</sup>

$$\beta_m = 2\pi \cos(\theta_{\text{inc}})/\lambda_m. \quad (6)$$

Taking into account that  $\theta_{\text{inc}} \ll 1$  { $\cos(\theta_{\text{inc}}) \approx 1 - \theta_{\text{inc}}^2/2$ }, we obtain from Eqs. (3) and (6)

$$\lambda_m = \theta_{\text{inc}}/(a_m)^{1/2}. \quad (7)$$

In wave optics a guided mode can be represented by a plane wave which reflects back and forth in a zigzag manner between the two surfaces of the film.<sup>6-8</sup> Then a definite angle  $\theta_m$  with the  $Z$  axis can be associated with the guided modes. These angles  $\theta_m$  can be defined from geometrical optics considerations as  $\cos(\theta_m) = \beta_m/kn_1$ , which yields to the following expression in using Eqs. (1) and (3):

$$\theta_m = \lambda_m(a_m - \delta_1)^{1/2}, \quad (8)$$

where we have used  $\cos(\theta_m) \approx 1 - \theta_m^2/2$ .

In a neutron thin-film waveguide composed by nonabsorbent materials, the losses are mainly due to the surface roughness. In general, the scattering losses caused by roughness can be described by two statistical parameters: the root mean square roughness (rms)  $\sigma$  given by Gaussian statistics and the height-height correlation length  $\xi$ .<sup>9,10</sup> In the case of total reflection the incoherent scattering can be neglected for small correlation lengths so only roughness with large correlation lengths contributes to the scattering losses. Thus the main effect of the roughness, if it is not periodic, comes from the rms  $\sigma$  corresponding to a decrease of the reflectivity in the specular direction by the Debye-Waller factor of the following form:  $\exp(-[4\pi\sigma \sin\theta/\lambda]^2)$ . Meanwhile the correlation length  $\xi$  mainly contributes to the scattering in other directions. In spite of some limitations,<sup>11</sup> the above formula is widely used because of its simplicity.<sup>8,12</sup> A more refined analysis of the influence of the roughness on the neutron reflectivity function is carried out in Refs. 9, 10, 13-15. The attenuation coefficient  $\alpha$  for neutron guided waves  $\{I(z) = I(0)\exp[-\alpha z]$ , where  $I(z)$  is the intensity of the guided neutron waves along the  $Z$  axis} can be evaluated as follows. On one zigzag of path, the neutron beam is displaced along the  $Z$  direction at a distance  $2h_{\text{eff}}/\tan(\theta_m)$  (Ref. 16) undergoing total reflection once from each interface. As defined by Eq. (8),  $\tan(\theta_m) = q_m/\beta_m$ . At a distance  $L$  the total number of reflections will be given by

$$N_{\text{tot}} = q_m L / (h_{\text{eff}} \beta_m). \quad (9)$$

From Eqs. (5) and (9)  $N_{\text{tot}}$  can be expressed as a function of the mode number:

$$N_{\text{tot}} = (m + 1) \lambda_m L / 2h_{\text{eff}}^2. \quad (10)$$

As can be seen the number of total reflections is linearly proportional to the mode number for low order modes. For a symmetrical waveguide, after a reflection from each interface the intensity is decreased by the Debye-Waller factor  $\exp\{-4q_m^2\sigma^2\}$ . So the attenuation coefficient  $\alpha$  can be easily found to be

$$\alpha = 4\sigma^2 q_m^2 N_{\text{tot}} / L, \quad (11)$$

which yields approximately to the following expression in using Eqs. (5) and (10):

$$\alpha \approx 2\pi^2 \sigma^2 \lambda_m (m + 1)^3 / h_{\text{eff}}^4. \quad (12)$$

If the roughness of two interfaces ( $\sigma_1$  and  $\sigma_2$ ) are not equal, then in formula (11)  $\sigma^2$  must be replaced by  $(\sigma_1^2 + \sigma_2^2)/2$ . Two important features of formula (12) are the mode number and the guiding layer thickness dependencies of the attenuation coefficient. As can be seen from formula (12),  $\alpha$  is a rapidly decreasing function of the effective height of the guide  $\alpha \sim 1/h_{\text{eff}}^4$ , so for the observation of neutron guided waves it is preferable to use guides with large effective thicknesses. The attenuation coefficient increase rapidly with the mode number as  $\alpha \sim (m + 1)^3$ , e.g., for the mode  $m=1$   $\alpha$  is approximately eight times greater than for the mode  $m=0$ . The transmitted intensity decreases with the mode number even faster  $I(L) = I(0)\exp\{-2L\pi^2\sigma^2\lambda_m(m + 1)^3/h_{\text{eff}}^4\}$ , where  $L$  is the length of the waveguide. Another interesting feature of the formula (12) is that  $\alpha$  is linearly proportional to the reso-

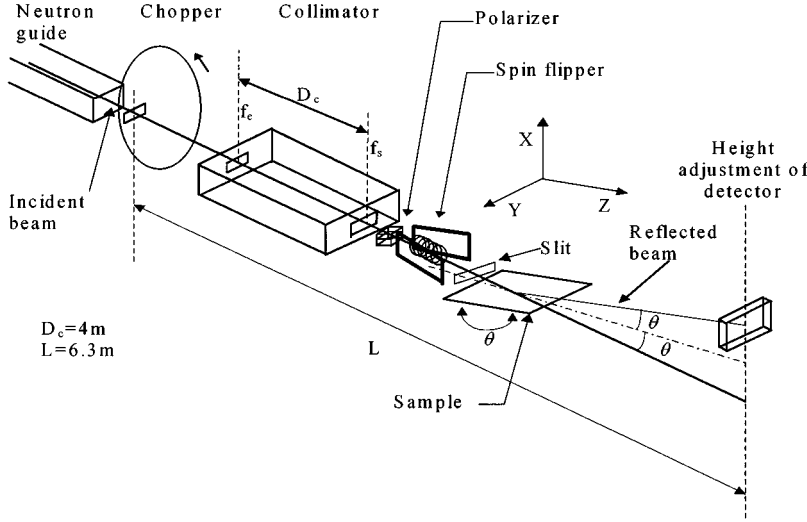


FIG. 2. Scheme of the EROS reflectometer with the polarizer and the spin flipper. The width of slits  $f_e$  and  $f_s$  was 2 mm. A third slit of 1 mm in height was installed in front of the sample after the spin flipper giving an angular resolution of  $0.04^\circ$ . For the polarized neutron experiment the polarizer, the spin flipper, and the slit before the sample were removed.

nant wavelengths  $\lambda_m$ . Meanwhile, according to Ref. 2 the intensity distribution of the neutron guided waves along the transverse  $X$  direction is wavelength independent, so it was “expected” that the guided wave field for any wavelength would “see” the roughness in the same manner. More details about the roughness, the coupling process, and the characteristic Eq. (2) one can find in Refs. 9, 10, 13–15, 2, 5, 7.

In our experiment the thin film is confined by CoZr which is a magnetic material. The magnetic moment in CoZr is directed in the positive direction of  $Y$  axis (Fig. 1). Then the spin-dependent refractive index of CoZr layers with the magnetic moment in the  $Z$ - $Y$  plane can be written in the following form:<sup>17</sup>

$$n_{\pm}^2 = 1 - \lambda^2(\delta \pm \gamma M), \quad (13)$$

where  $\gamma$  is a constant ( $0.844 \times 10^{-13} \mu_B/\text{cm}$ ), and  $M$  is the magnetic moment of saturation.  $n_{\pm}$  are spin-dependent refractive indices, indicating respectively that the neutron spin is either parallel (up) or antiparallel (down) to the magnetization direction.  $\delta$  is related to the refractive index of non-polarized neutrons by Eq. (1). The values of  $\delta$  and  $\gamma$  for different materials one can find in many neutron optics textbooks, e.g., in Refs. 17, 18.

Since the refractive indices  $n_1$  of Al guiding film is between,  $n_+ < n_1 < n_-$ , then the resonance condition is satisfied only for up polarization. The total reflection condition is not satisfied for down polarized neutrons, so they undergo high attenuation losses due to the multiple reflections from GGG absorbing substrate.

### III. SAMPLE PREPARATION AND REFLECTIVITY MEASUREMENTS

The experimental setup scheme is described in Fig. 1. The multilayer CoZr/Al/CoZr/GGG was produced by the rf sputtering starting of 10 in. diameter CoZr and Al targets in a Z550 Leybold-Heraeus system for an argon working pressure of  $2.5 \times 10^{-2}$  mbar. A single crystal (111) oriented rectangular substrate  $20 \times 64 \text{ mm}^2$  of gadolinium-gallium garnet ( $\text{Gd}_3\text{Ga}_5\text{O}_{12}$  or GGG) was used due to the high neutron absorption coefficients of the  $\text{Gd}^{3+}$  ions and the very low roughness of the high polished surface (roughness  $< 5 \text{ \AA}$ ).

This ensures that in the transmitted intensity measurement no intensity is reflected by the substrate. The sandwich structure  $\text{Co}_{0.95}\text{Zr}_{0.05}/\text{Al}/\text{Co}_{0.95}\text{Zr}_{0.05}$  was prepared from the deposition of the first 1300  $\text{\AA}$  thick  $\text{Co}_{0.95}\text{Zr}_{0.05}$  layer followed by a 2800  $\text{\AA}$  thick Al film and finally by the second  $\text{Co}_{0.95}\text{Zr}_{0.05}$  layer. The first 1300  $\text{\AA}$  thick CoZr layer is used to isolate the neutrons guided waves from the GGG absorbing substrate [the guided neutrons efficient evanescent penetration length in CoZr is of the order of 320  $\text{\AA}$  (Ref. 2)]. The last CoZr layer is of step shape (Fig. 1) with very thin extremities (100  $\text{\AA}$  thick) for in/out coupling of incident neutrons into Al guiding film and the thick part (1500  $\text{\AA}$  thick, 6 mm long) providing a symmetrical form for the waveguide. The latter prevents the neutrons leakage back to air. In order to absorb the neutrons reflected from the left hand prism region,  $\text{B}_4\text{C}$  powder of 5 mm height have been deposited on top of the middle  $\text{Co}_{0.95}\text{Zr}_{0.05}$  step (Fig. 1).

In order to characterize the sample, polarized neutrons reflectivity measurements have been performed using the time of flight reflectometer EROS installed on the Orphée reactor at the Laboratoire Léon Brillouin at Saclay. A sketch of this reflectometer is shown in Fig. 2. The chopper produces neutrons pulses of 240  $\mu\text{s}$  duration leading to a wavelength resolution of 0.1  $\text{\AA}$ . A flipping ratio of more than 20 was measured on the wavelength range of 5 to 15  $\text{\AA}$ . Along the  $Y$  axis a magnetic field of 300 Oe was applied to the sample in order to ensure the saturation of the CoZr layers. For each spin state the measurements were performed at incidence angles:  $\theta_{\text{inc}} = 0.3^\circ, 0.6^\circ, \text{ and } 1.2^\circ$ . The results of neutron reflectivity are shown in Fig. 3 and are in a good agreement with simulations using the classical reflectivity approach.<sup>19</sup> The best fit values of the waveguide parameters are presented in Table I.

Transmitted intensity through the thin film of Al has been measured with nonpolarized neutrons using an angle of incidence  $\theta = 0.3^\circ \pm 0.005^\circ$ . Similarly to the polarized neutron measurements, the sample was placed in a magnetic field of 300 Oe along the  $Y$  direction. In order to obtain higher intensity, the polarizer, spin flipper, and the slit before the sample were removed. For transmitted resonance measurements width of 0.5 mm was used for slits  $f_e$  and  $f_s$  (Fig. 2)

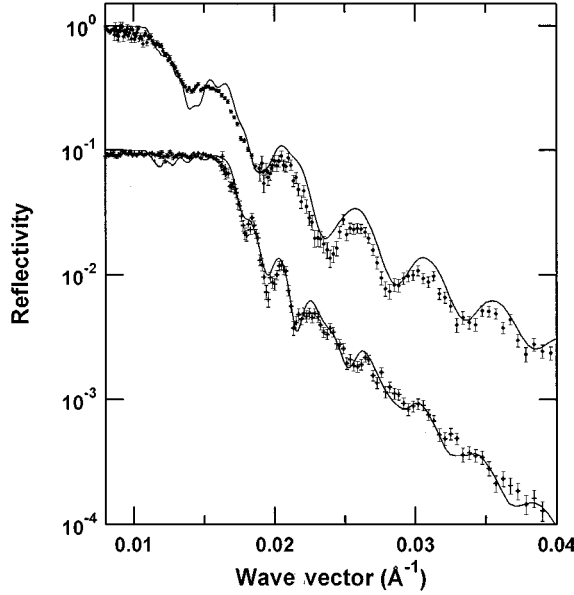


FIG. 3. Scattered wavevector  $\{Q=4\pi \sin(\theta)/\lambda\}$  dependence of the reflectivity function for two spin states. Measurements and simulations (solid lines) for the spin up state are shifted by a factor of 10 for clarity. For each spin state the measurements performed at  $\theta=0.3^\circ$ ,  $0.6^\circ$ , and  $1.2^\circ$  have been brought together.

leading to an angular resolution of  $0.01^\circ$ . In these particular conditions we obtain a wave vector resolution of  $0.0007 \text{ \AA}^{-1}$ . A transmitted resonant intensity was measured at  $Q_{\text{trans}}=0.0111 \pm 0.0004 \text{ \AA}^{-1}$  (Figs. 4 and 5).  $Q$  is the scattered wave vector defined as  $Q=4\pi \sin(\theta_{\text{inc}})/\lambda$ . From Eqs. (3) and (7) it is easy to obtain the following expression for  $Q_m$  corresponding to the guided modes:

$$Q_m = 4\pi(a_m)^{1/2}. \quad (14)$$

Apparently  $Q_m$  are wavelength independent for guided waves, since  $a_m$  are wavelength independent determined from Eq. (4). In using the values of parameters obtained by the fit to the reflectivity spectra for three different incidence angles (Fig. 3),  $Q_m$  are evaluated in Table I by Eq. (14).

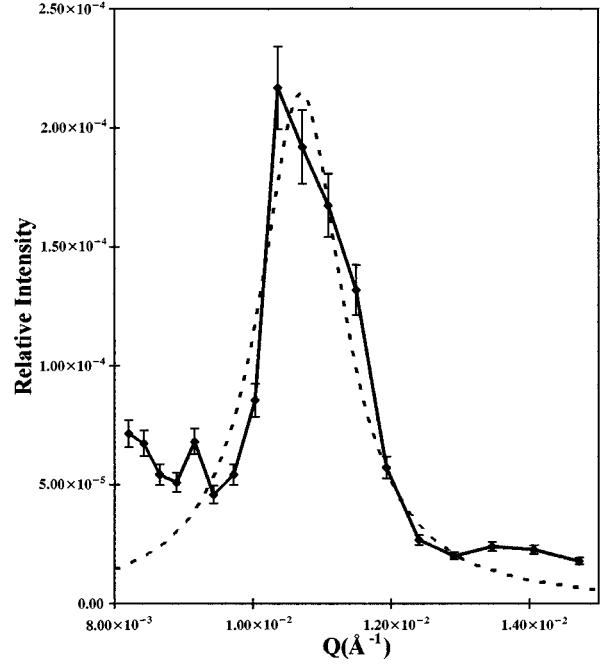


FIG. 4. Dependence of the scattered wavevector  $Q$  on the ratio of the transmitted intensity divided by the incident intensity (solid line). The transmitted resonance is fitted by a single Lorentzian line shape (dotted line).

#### IV. DISCUSSIONS

In Table I the values of the waveguide parameters obtained by a fit to the reflectivity data are presented. It is well known that the inverse refractive index profile calculation from the reflectivity data has serious limitations since the phase information is missing.<sup>19,20</sup> The lack of the phase information leads to an infinite number of solutions giving the same reflected intensity pattern. The influence of the background intensity and the experimental errors on the precision of the waveguide parameters determination are in general ignored. Meanwhile the problem is ill posed and the small variations of the reflectivity data produce generally strong variations of the inverse problem solution.<sup>20</sup> This is why the

TABLE I. In the first column the best fit values of the waveguide parameters are presented. In the second, third, fourth, and fifth columns are given the resonant scattered wavelength, the number of modes, the propagation angle in the guide, and the transmission quality parameter, respectively.  $\delta_j$  are related to the refractive index of neutron waves by Eq. (1).  $\delta^\pm = \delta \pm \gamma M$  are given by Eq. (11) and are related to  $n_\pm$  by  $n_\pm^2 = 1 - \lambda^2 \delta^\pm$ .

Best fit values of waveguide parameters	Scattered wavevector $Q_m = 4\pi(a_m)^{1/2}$	Number of total reflections $N_{\text{tot}}$	Propagation angle in the guide $\theta_m$ (deg)	Transmission quality $\kappa(L) = I_{\text{inc}}/I_{\text{trmsm}}$
$\delta_{\text{Al}} = 6.68 \times 10^{-7} \text{ \AA}$	$Q_0 = 0.0105$	19	0.058	0.908
$\delta_{\text{CoZr}} = 1.78 \times 10^{-6} \text{ \AA}$	$Q_1 = 0.0110$	37	0.110	0.481
$h_{\text{Al}} = 2810 \text{ \AA}$	$Q_2 = 0.0119$	51	0.152	0.105
$h_{\text{CoZr}} = 1300 \text{ \AA}$	$Q_3 = 0.0130$	61	0.185	0.008
$d_{\text{CoZr}} = 100 \text{ \AA}$	$Q_4 = 0.0143$	67	0.209	$2.9 \times 10^{-4}$
$L = 6 \text{ mm}$	$Q_5 = 0.0157$	68	0.227	$8.1 \times 10^{-6}$
$\sigma = 45 \text{ \AA}$				

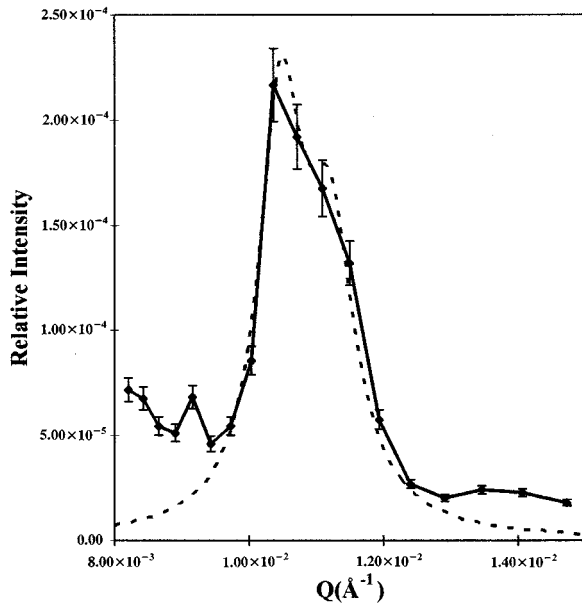


FIG. 5. Dependence of the scattered wavevector  $Q$  on the ratio of the transmitted intensity divided by the incident intensity (solid line). The transmitted resonance is fitted by double Lorentzian lines (dotted line).

optimization procedure provides several sets of waveguide parameters each corresponding to a local minimum of the optimization function. From a few solutions corresponding to the same order local minima of the optimization function we have chosen in the Table I the set which corresponds the better to the values ‘‘expected’’ by the waveguide fabrication technique. While the refractive index of Al obtained by the fitting procedure is close to its usual tabulated value,<sup>18</sup> the refractive index of the CoZr layers are much smaller than their tabulated value. The thicknesses of the Al and CoZr layers agree well with their values estimated from the sputtering time considerations. In Table I we bring in also the values of different parameters of the waveguide figuring in formulas (8)–(12).

Interesting results are obtained when the experimental transmitted resonance curve is fitted to one or double Lorent-

zian lines. A fit to a single Lorentzian line shape (Fig. 4) gives a resonance centered at  $Q_{\text{Lor}}=0.0107 \text{ \AA}^{-1}$  with a full width at half maximum  $\Delta Q_{\text{Lor}}=0.00073 \text{ \AA}^{-1}$ . As can be seen the resonance value is slightly shifted from the value obtained from theoretical estimations (Table I).

The asymmetrical shape of the transmitted resonance suggests a fit to a sum of several Lorentzian curves. However, the poor experimental resolution allows the experimental data to be approximated only by two Lorentzian forms with following parameters. The first resonance is centered at  $Q_{\text{Lor}}=0.0105 \text{ \AA}^{-1}$  with a full width at half maximum  $\Delta Q_{\text{Lor}}=0.00039 \text{ \AA}^{-1}$  (Fig. 5) and the second resonance is centered at  $Q_{\text{Lor}}=0.0112 \text{ \AA}^{-1}$  with a full width at half maximum  $\Delta Q_{\text{Lor}}=0.00045 \text{ \AA}^{-1}$  (Fig. 5). As can be seen from Fig. 5 and Table I the peak locations of Lorentzian lines agree remarkably well with the evaluated values of the first two low order guided modes. The third mode is at the edge of the experimentally observed resonance region. Indeed the third and other higher order modes are subject to high attenuation losses due to the surface roughness as seen from Table I. So only the first two low order modes are really observable as confirmed by the experiment. For the first two low order modes the number of reflections on 6 mm guide length are evaluated on Table I to be  $N_{\text{tot}}=19$  and 37, respectively. In order to estimate the attenuation losses due to the surface roughness, let us evaluate the waveguide transmission quality parameter defined as  $\kappa(L)=\exp(-\alpha L)$ , where  $L$  is the length of the waveguide. The transmission quality parameter  $\kappa(L)$  shows how many times the in coupled intensity is decreased after the propagation in the guide a distance  $L$ . In using the values of different parameters of the guide given in Table I and the resonance position value  $Q_{\text{Lor}}$ , the  $\kappa(L)$  is estimated for the first mode ( $m=0$ ) to be 0.908 corresponding to a mean roughness  $\sigma=[(\sigma_1^2+\sigma_2^2)/2]^{1/2}\approx 35 \text{ \AA}$ . For the second and third modes ( $m=1$  and 2),  $\kappa(L)$  are respectively 0.481 and 0.105. Obviously, even if the high order modes are effectively coupled into the waveguide, they will undergo high attenuation losses due to the scattering on the surface roughness. This is why we observe only the first two low order modes in the transmittivity spectrum.

In conclusion, we have observed two transmitted guided bound modes in a multilayer CoZr/Al/CoZr sandwich in a good agreement with theoretical predictions.

<sup>1</sup>R. E. De Wames and S. K. Sinha, Phys. Rev. B **7**, 917 (1973).  
<sup>2</sup>S. P. Pogossian and H. Le Gall, Opt. Commun. **114**, 235 (1995).  
<sup>3</sup>Y. P. Feng, C. F. Majkrzak, S. K. Sinha, D. G. Wiesler, H. Zhang, and H. W. Deckman, Phys. Rev. B **49**, 10 814 (1994).  
<sup>4</sup>S. P. Pogossian, thesis, Université de Brest, 1994.  
<sup>5</sup>S. P. Pogossian, H. Le Gall, and A. Menelle, J. Magn. Magn. Mater. **152**, 305 (1996).  
<sup>6</sup>T. Tamir, *Integrated Optics* (Springer-Verlag, Berlin, 1971).  
<sup>7</sup>R. Ulrich, J. Opt. Soc. Am. **60**, 1337 (1970).  
<sup>8</sup>P. K. Tien, Appl. Opt. **10**, 2395 (1971).  
<sup>9</sup>S. K. Sinha, E. B. Sirota, S. Garoff, and H. B. Stanley, Phys. Rev. B **38**, 2297 (1988).  
<sup>10</sup>D. K. G. de Boer, Phys. Rev. B **51**, 5297 (1995).  
<sup>11</sup>P. Beckmann and A. Spizzichino, *International Series of Mono-*

*graphs on Electromagnetic Waves* (Oxford University Press, New York, 1963).  
<sup>12</sup>B. A. Vidal and J. C. Marfaing, J. Appl. Phys. **65**, 3453 (1989).  
<sup>13</sup>L. Nénot and P. Croce, Rev. Phys. Appl. **15**, 761 (1980).  
<sup>14</sup>B. Vidal and P. Vincent, Appl. Opt. **23**, 1794 (1984).  
<sup>15</sup>R. Pynn, Phys. Rev. B **45**, 602 (1992).  
<sup>16</sup>R. Ulrich and W. Prettl, Appl. Phys. **1**, 55 (1973).  
<sup>17</sup>V. F. Sears, *Neutron Optics* (Oxford University Press, New York, 1989), pp. 89–96.  
<sup>18</sup>Neutron News **3**, 26 (1992).  
<sup>19</sup>T. P. Russel, Mater. Sci. Rep. **5**, 171 (1990).  
<sup>20</sup>A. Roger, D. Maystre, and M. Cadilhac, J. Opt. (Paris) **9**, 83 (1978).